

# Rapid Intradermal Delivery of Liquid Formulations Using a Hollow Microstructured Array

Scott A. Burton · Chin-Yee Ng · Ryan Simmers · Craig Moeckly · David Brandwein · Tom Gilbert · Nathan Johnson · Ken Brown · Tessa Alston · Gayatri Prochnow · Kris Siebenaler · Kris Hansen

Received: 25 February 2010 / Accepted: 19 May 2010  
© The Author(s) 2010. This article is published with open access at Springerlink.com

## ABSTRACT

**Purpose** The purpose of this work is to demonstrate rapid intradermal delivery of up to 1.5 mL of formulation using a hollow microneedle delivery device designed for self-application.

**Methods** 3M's hollow Microstructured Transdermal System (hMTS) was applied to domestic swine to demonstrate delivery of a variety of formulations including small molecule salts and proteins. Blood samples were collected after delivery and analyzed via HPLC or ELISA to provide a PK profile for the delivered drug. Site evaluations were conducted post delivery to determine skin tolerability.

**Results** Up to 1.5 mL of formulation was infused into swine at a max rate of approximately 0.25 mL/min. A red blotch, the size of the hMTS array, was observed immediately after patch removal, but had faded so as to be almost indistinguishable 10 min post-patch removal. One-mL deliveries of commercial formulations of naloxone hydrochloride and human growth hormone and a formulation of equine anti-tetanus toxin were completed in swine. With few notable differences, the resulting PK profiles were similar to those achieved following subcutaneous injection of these formulations.

**Conclusions** 3M's hMTS can provide rapid, intradermal delivery of 300–1,500  $\mu$ L of liquid formulations of small molecules salts and proteins, compounds not typically compatible with passive transdermal delivery.

**KEY WORDS** transdermal drug delivery · microneedles · intradermal · hollow microstructures · MTS

S. A. Burton · C.-Y. Ng · R. Simmers · C. Moeckly · D. Brandwein · T. Gilbert · N. Johnson · K. Brown · T. Alston · G. Prochnow · K. Siebenaler · K. Hansen (✉)  
3M Drug Delivery Systems Division  
Building 260-03-A-05  
St. Paul, Minnesota 55114, USA  
e-mail: kjhansen@mmm.com

## INTRODUCTION

Transdermal patches have long been used for the administration of small-molecule lipophilic drugs that can be readily absorbed through the skin. This non-invasive delivery route is advantageous for the administration of many drugs incompatible with oral delivery, as it allows for direct absorption of the drug into the systemic circulation, by-passing both the digestive and hepatic portal systems which can dramatically reduce the bioavailability of many drugs. Transdermal delivery also overcomes many of the challenges associated with subcutaneous injection by greatly reducing patient discomfort, needle anxiety, risk of accidental needle stick injury to the administrator and issues surrounding sharps disposal (1,2).

Despite these many advantages, transdermal delivery of drugs is confined to classes of molecules compatible with absorption through the skin. Delivery of small molecule salts and therapeutic proteins are not typically viable with traditional transdermal delivery, as the skin provides an effective protective barrier to these molecules even in the presence of absorption-enhancing excipients (2).

The use of microstructure- or microneedle-assisted transdermal delivery has long been proposed as a means of capitalizing on the benefits of, while simultaneously mitigating the challenges associated with, traditional transdermal delivery. Small needles or projections, usually less than 2 mm in length, can be inserted into the skin with minimum patient discomfort and, given the small hole created, with minimal risk of post-injection infection, bleeding, or risk of inadvertent IV injection for an intradermal administration. In addition, microneedles reduce risk to the injection administrator, as accidental puncture of the skin is nearly impossible with these small projections (3).

Delivery of drugs using both solid and hollow micro-needles has been demonstrated and described in the technical literature (4–9). In 2007, Haq *et al.* conducted a study on healthy volunteers comparing the injection pain and resulting tissue damage between two different types of microneedles, and a 25-gauge hypodermic needle. Study subjects reported significantly less pain upon injection with the microneedles, and researchers noted that skin trauma was less and injection site healing was faster with microneedles (4). In a 2002 study, researchers at Becton Dickinson (BD) Technologies reported the results of a human clinical study demonstrating delivery of vaccines using flat-headed, solid microneedles. Effective delivery of vaccine was demonstrated with minimal discomfort or skin irritation noted by the clinical subjects (5).

In 2003, McAllister *et al.* reported injection of up to 32 microliters ( $\mu\text{L}$ ) of insulin into hairless rats with induced diabetes using a glass microneedle device. In this study, a single glass microneedle was drilled into the dorsal skin, and the insulin formulation was infused at a pressure of 10 lbs per square inch (psi) over 30 min. Analysis of blood samples indicated a statistically significant and dose-dependent drop in blood glucose levels over a 5-h period (6). A similar study was conducted by Nordquist *et al.* using a microneedle-based infusion patch to deliver insulin to rats to provide glycemic control (7).

More recently, a microneedle-based syringe device has been utilized for intradermal delivery of influenza vaccines. Successful administrations of 100 and 200  $\mu\text{L}$  doses of the vaccine were achieved in human patients. Although local site reactions were more frequent in the intradermal group when compared to the IM injection group, these reactions were mild and transient (8). In 2009, delivery of insulin to diabetic human patients was demonstrated using a single microneedle inserted into the skin using a custom-made rotary drilling device. The max volume delivered in this study was approximately 300  $\mu\text{L}$  administered at a rate of 1,000  $\mu\text{L}/\text{min}$  (9).

Biopharmaceuticals are pharmaceutical compounds derived from human, animal or microbial sources (4). According to the pharmaceutical research firm, IMS Health, global sales of biologics rose over 12% in 2007, a growth rate roughly double that of classic small-molecule-based pharmaceutical products; biopharmaceuticals account for 25% of the pharmaceutical development pipeline (10). Recent estimates indicate that the demand for biopharmaceutical products rose to nearly \$70 billion in 2008. Monoclonal antibodies, the fastest growing class of biopharmaceutical compounds, are generally engineered to target specific diseases such as cancer, macular degeneration and rheumatoid arthritis (11).

The production of biopharmaceuticals is extremely resource intensive, and as a result, biopharmaceuticals are often significantly more costly than traditional chemical pharmaceuticals. For this reason, high efficiency, from

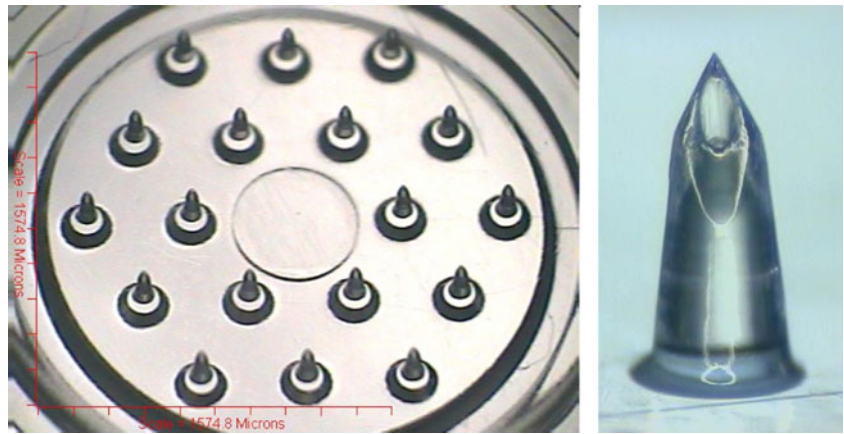
production in the manufacturing facility through delivery to the patient, is required (10). The vast majority of biopharmaceutical products currently have dosing requirements in excess of 0.5 mL; these volume requirements place added burdens on the delivery system as they outstrip the capabilities of many delivery technologies (11). The efficiency and volume demands, coupled with the relative instability of these protein- and peptide-based molecules, mean that biopharmaceuticals are nearly universally incompatible with oral, inhalation or traditional transdermal delivery technologies. They typically require administration via a syringe injection or IV infusion (12), delivery options that can cause pain, deep tissue trauma, and anxiety—all factors that may adversely effect patient compliance. Although much progress has been made in the development of microneedle-based systems for transdermal delivery, most commercially viable devices that provide intradermal delivery of liquid formulations remain confined to relatively small volumes, typically  $< 200 \mu\text{L}$ .

The 3M hollow Microstructured Transdermal System (hMTS) is designed to allow relatively pain-free and fast intradermal delivery of a high volume of a liquid drug formulation to the highly vascularized dermal layer of skin. The hMTS array is a disk comprised of evenly spaced microneedles connected to a conventional glass cartridge. Delivery of the liquid formulation through the microstructures is powered by a spring. The device applies the microstructures into the skin to a depth sufficient to penetrate the stratum corneum and the epidermis and create direct access to the dermis.

The hMTS is a fully integrated microneedle delivery device designed for self administration. The volume capabilities of the device exceed those of traditional ID injection and make the hMTS device a viable delivery option for many biopharmaceutical therapeutics currently available for delivery only with a conventional syringe or an autoinjector. The hMTS system provides efficient, intradermal delivery of pharmaceutical formulations of 0.5–1.5 mL. The delivery time is on the order of minutes *versus* seconds (as is needed for a syringe or auto injector), and the delivery surface is spread across a  $1 \text{ cm}^2$  array *versus* a single point source provided by a syringe.

During *in vivo* studies in swine, the hMTS device was used to deliver 1,500  $\mu\text{L}$  of placebo formulation in as little as 2–6 min. A red, array-sized blotch and a small wheal or dome is observed immediately after patch removal, but fades so as to be almost indistinguishable within 10 min post-patch removal; the wheal is resolved to the touch after about 40 min post-infusion. Deliveries of up to 1,500  $\mu\text{L}$ , using delivery rates up to 100  $\mu\text{L}/\text{min}$ , were repeated using a dilute isotonic methylene blue solution to enable visualization of the delivery. Delivery of a 1  $\mu\text{g}/\text{mL}$  commercial formulation of naloxone, a 2 mg/mL formulation of hGH and a 57 mg/mL formulation

**Fig. 1** hMTS polymeric microneedle array and a single microstructure.



of a polyclonal antibody were also demonstrated. Blood samples collected and analyzed after delivery indicate PK profiles similar to those achieved following administration of the same amount of formulation by subcutaneous injection.

**MATERIALS AND METHODS**

**Microneedle Array and Integrated Delivery Device**

The polymeric hMTS array (3M, St. Paul, MN) is 1.27 cm<sup>2</sup> and consists of eighteen 500–900 μm microstructures shaped like mini-hypodermic needles. Each structure has a 10–40 μm cannula that allows fluid communication between the microstructures and the back of the array (Fig. 1).

The array is integrated into the device which includes an application spring, a glass cartridge API reservoir and a spring for delivery. The device is held to the skin with an adhesive patch and is designed to be worn on the upper arm or upper thigh (Fig. 2).

**Animal Models and Skin Preparation**

*Hairless Guinea Pigs (HGP)*

Male HGPs were ordered from Charles River Laboratories (Wilmington, MA) under a 3M IACUC-approved animal

use application and used according to that protocol. All animals used in this study weighed 0.8–1 kg. HGPs were used to characterize the depth of penetration associated with the microstructures.

*Domestic Swine*

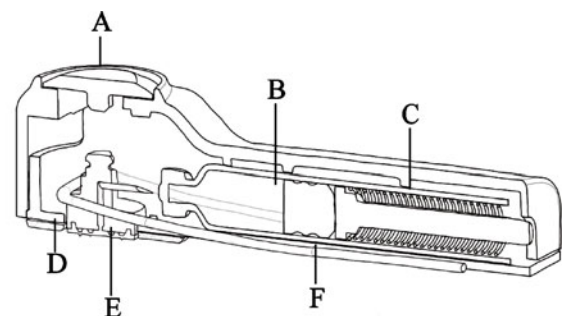
Testing was conducted on female domestic swine approximately 6–18 weeks old and weighing approximately 10–35 kg, obtained under a 3M IACUC-approved animal use application. During delivery and throughout the studies, the swine were maintained under anesthesia with an isoflurane (2–5%) oxygen mix. Deliveries were performed on the ham of the swine which was shaved first using a surgical clipper (clip blade #50) and then with a Schick 3 razor using a small amount of Gillette Foam shaving cream. After shaving, the site was rinsed with water, patted dry and then wiped with iso-propyl alcohol (Phoenix Pharmaceutical, Inc., St. Joseph, MO).

**Penetration Experiments**

*Microstructure Preparation and Evaluation*

To prepare the microstructures for depth of penetration (DOP) determination, the hMTS arrays were coated with 45 μl of a 0.08% w/v Rhodamine B dye (Sigma Aldrich, St.

**Fig. 2** hMTS integrated device which includes **A** actuator, **B** glass injection cartridge, **C** delivery spring, **D** adhesive, **E** hollow microstructured array, and **F** application spring.



Louis, MO) solution in water and oven dried at 35°C for 30 min. The arrays were inserted in to the HGP and swine and allowed to remain in the animals for 10 min before removal. The structures were imaged under bright field microscopy before and after array application using a Nikon ME600 microscope (Nikon, Melville, NY) equipped with a digital camera and Image Pro Plus software (Media Cybernetics, Inc., Bethesda, MD). Image Pro Plus allows for measurement of the distance from the tip of the microstructure to the point on the microstructure where the Rhodamine B dye is no longer wiped off due to insertion into the skin. All images were captured using the 10× magnification eyepiece.

To ensure sufficient durability of the microstructures, the array was pressed against a non-elastic surface with increasing amounts of weight. Upon removing the array from the skin, the arrays were inspected microscopically to evaluate the integrity of the microstructures.

### **Methylene Blue Staining**

Penetration of the stratum corneum by the microstructures was assessed by staining the application site with a methylene blue solution after removal of the array. Once the array was removed, a hilltop chamber was attached to the skin immediately surrounding the application site. The chamber was filled with a mixture of 2 mg/mL methylene blue (Aldrich, Milwaukee, WI) and 0.02 mg/ml Tween 80 in water. The dye/Tween mix was allowed to stay in contact with the skin for 10 min. At the end of the staining period, the chamber was removed and the skin site cleaned with water. A photograph of the site was taken upon removal of the hilltop chamber to document the effect of staining.

### **Delivery Experiments**

#### **Dextrose**

General characterization of delivery parameters was completed using a 5% Dextrose, USP, solution for injection (Baxter Healthcare, Deerfield, IL); the solution was used as received.

#### **Methylene Blue**

The 0.001% methylene blue solution (Aldrich, Milwaukee, WI) was prepared using sterile water and was filtered prior to administration.

#### **Naloxone**

A commercial formulation (1 mg/mL) of naloxone hydrochloride (International Medication Systems, Ltd., So. El Monte, CA) was used for hMTS delivery and injection.

### **Human Growth Hormone**

The hGH (Calbiochem, Trenton, NJ) was formulated at 2 mg/mL with 5% dextrose in water prior to delivery. The hGH administered by injection was the commercial formulation Humatrope (Lilly France, SAS, Fergersheim, France), also a 2 mg/mL formulation.

### **Equine Tetanus Anti-Toxin (ETAT)**

A polyclonal IgG formulation was developed as a model for a therapeutic monoclonal antibody. Filtered horse serum containing high levels of anti-tetanus toxin antibodies (Colorado Serum Company, Denver, CO) was processed using Protein-A to create an IgG-polyclonal pool. This fraction was sterile filtered then aseptically concentrated and buffer exchanged to a final concentration of 57 mg/mL IgG in 4.25% dextrose and 75 mM NaCl. This antibody concentration is in the range of commercial monoclonal antibody formulations, such as Humira® (Abbott), currently administered as a 50 mg/mL injectable.

### **Injection Experiments**

The same formulations used for delivery via hMTS were administered to the swine via subcutaneous injection using a 23-gauge needle and 1-mL syringe. In all cases, the subcutaneous injections were administered behind the right shoulder of the swine.

### **Serum Naloxone Determination**

At each time point, 1.5–2 mL of whole blood was collected from the ear vein of the swine using a Vacutainer Collections Set (Becton Dickenson & Co., Franklin Lakes, NJ). The blood was allowed to set at room temperature for at least 30 min prior to being centrifuged at 1,500 rpm for 10 min. After centrifugation, the serum was separated from the whole blood and stored cold until extraction.

Room temperature serum samples were prepared using solid phase extraction cartridges (Phenomenex, Torrance, CA). Cartridges were conditioned with methanol (EMD Chemicals, Inc., Gibbstown, NJ) and equilibrated with reagent grade water before loading with the serum samples. Serum was washed with 2 mL of 5% methanol in reagent grade water and naloxone eluted with 100% methanol. The eluent was collected in a 14 mL glass tube or a 16×100 mm tube and dried under 15 psi of nitrogen in a 37C water bath.

Extracts were reconstituted with 5% acetonitrile/95% 0.1% formic acid (Alfa Aesar, Ward Hill, MA) in water, transferred to microcentrifuge tubes (Eppendorf, Westbury, NY) and centrifuged at 14,000 rpm for 10 min.

Extracts were quantitatively analyzed using LCMSMS. Separation was achieved using an Agilent Eclipse XDB-C18 column (Agilent Technologies, Wilmington, DE) in sequence with a Phenomenex C18 Guard Column (Phenomenex, Torrance, CA); the mobile phase was 0.1% formic acid and acetonitrile; the formic acid was ramped from 95% to 10% over 1 min. A Sciex API3000 triple quad mass spectrometer (Applied Biosystems, Foster City, CA) running in positive ion mode using a Turbo IonSpray interface was used to quantitatively monitor the product ions resulting from the following  $m/z$  transitions: 328.17→310.10 and 342.16→324.30. The linear range for naloxone was 0.1 to 100 ng/mL evaluated using a 1/x curve weighting.

Various sizes of swine were dosed, so to normalize blood naloxone levels with respect to swine weight, the blood naloxone levels were multiplied by a conversion factor of 62 mL blood/kg of swine weight and then multiplied by the weight of the swine at dosing (kg). Final results are plotted as  $\mu\text{g}$  naloxone/swine.

### Serum hGH Determination

At each time point, approximately 2 mL of whole blood was collected from the ear vein of the swine using a Vacutainer Collections Set and transferred into a Serum Separator Tube (Becton Dickinson & Co., Franklin Lakes, NJ). The blood was allowed to clot at room temperature for at least 30 min prior to being centrifuged 1,000 $\times$ g for 15 min at 4°C. Serum was stored  $\leq$ -20°C until analysis.

Serum samples were analyzed using an appropriate ELISA kit (Quantikine hGH Immunoassay, R&D Systems, Minneapolis, MN) as per instructions packaged with the kit.

### Serum ETAT Determination

At each time point, 3 mL of whole blood was collected from the ear vein of the swine using a Vacutainer Collections Set and transferred into a Serum Separator Tube (Becton Dickinson & Co., Franklin Lakes, NJ). The blood was allowed to clot at room temperature for at least 30 min prior to being centrifuged at 3,000 rpm for 10 min. Serum was frozen on dry ice and stored  $\leq$ -20°C until analysis.

Serum samples were analyzed for equine anti-tetanus IgG using an ELISA developed in house. Briefly, 96-well MaxiSorp™ microtiter plates (Nunc Thermo Fisher Scientific, Rochester, NY) were coated overnight with tetanus toxoid for *in vitro* use (Statens Serum Institute, Copenhagen, DK) at 0.23 Lf per well in 50 mM carbonate-bicarbonate buffer pH 9.6 (Sigma, St Louis, MO) and blocked with 0.1% ELISA-grade bovine serum albumin

(Calbiochem EMD Biosciences, San Diego, CA) diluted in phosphate-buffered saline (PBS; HyClone Thermo Fisher Scientific, Waltham, MA). Plates were washed with PBS, 0.05% Tween 20 (Sigma, St. Louis, MO). Serum samples were applied and plates incubated for 2 h at 37°C. Plates were washed and incubated with rabbit anti-equine IgG (H + L)-horseradish peroxidase conjugate (GeneTex, Irvine, CA) at 37°C for 1 h. Plates were washed again, and 3,3',5,5'-Tetramethylbenzidine Substrate Solution (Calbiochem) was applied. Color was allowed to develop for 10–20 min, then stopped by application of 1N H<sub>2</sub>SO<sub>4</sub>. Plates were read at 450 nm using a SpectraMax 384Plus (MDS Molecular Devices, Sunnyvale, CA). Anti-toxin units were read off of a standard curve of filtered commercial Tetanus Anti-Toxin, Equine Origin (Professional Biological Supply, Denver, CO) diluted in normal porcine serum (in-house reagent) run on each plate. Undiluted standard was assigned a concentration of 300 anti-toxin units/mL.

## RESULTS

### Penetration and DOP in HGPs and Swine

Based on the technical literature, and considering the size of the microstructures, it was determined that a force of 0.004–0.16 N per microstructure is required for penetration of the stratum corneum (13). With the hMTS array, tip bending occurred when approximately 245 N of force was applied to the array (18 structures). Microscopic inspection of the arrays following *in-vivo* insertion was conducted; no structures were fractured or broken off of the array.

Figure 3 shows an application site on a HGP after patch removal before and after staining with methylene blue; the red color in Fig. 3a is due to staining from the Rhodamine B dye coated on the microstructures prior to application; no blood was observed during or after application.

The penetration of the stratum corneum by each of the 18 microstructures is evident from the pattern of blue dots in Fig. 3b.

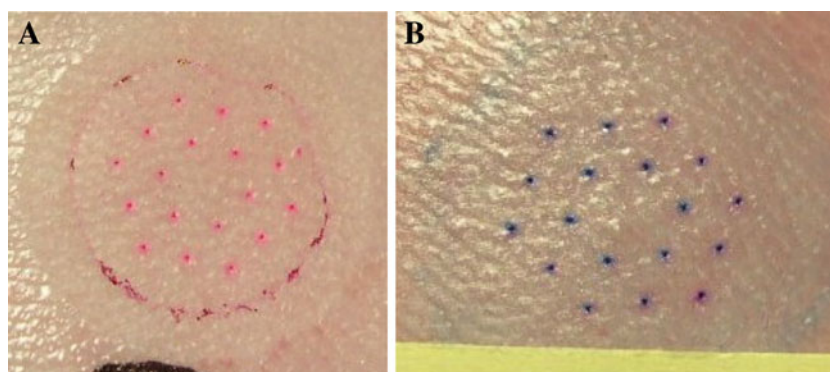
The DOP experiments were completed for the 500  $\mu\text{m}$  structures in both HGPs and in domestic swine and in domestic swine for the 900  $\mu\text{m}$  structures; the results from the insertion studies are summarized in Table I.

For the 900  $\mu\text{m}$  structures applied into swine, the average inter-array variability was 12% and ranged from 7–23%.

### Visual Site Assessment

Although HGPs are an appropriate model for characterization of DOP, these animals do not have sufficient surface

**Fig. 3** HGP skin after hMTS patch removal and before **a** (red color is due to Rhodamine B coated on the microstructure prior to application) and **b** after staining of the site with methylene blue.



vasculature for easy blood sampling and thus are not easily amenable to the development of a PK profile. Some studies cited in the literature utilize a rat model (6, 7), but these studies provide a poor correlation to human skin both with respect to dermal thickness and physiology. The domestic swine was chosen for the important dermal physiologic similarities to humans. Additionally, the domestic swine demonstrates similar intradermal pharmacokinetics to humans (14).

Several infusions of up to 1.5 mL were conducted using a sterile 5% dextrose or 0.001% methylene blue solution. Once the formulation had been delivered, the device was allowed to stay in place for up to 10 min to minimize the potential for leaking. Figure 4 shows the results of an 800  $\mu$ L intradermal infusion of a 0.001% methylene blue formulation into swine.

The skin is dry to the touch after patch removal; the deep blue of the infused formulation provides a visual assessment of the treatment. Each blue spot on the skin corresponds to one of the eighteen hollow microstructures on the array. Although the dye appears somewhat smeared (diffused) after 9 min, the blue stain remained, essentially unchanged 24 h later, although the wheal disappeared in under an hour. It is likely that the dye stains the tissue and, in this sense, is probably not an effective indicator of intradermal infusion patterns post delivery.

Figure 5 shows skin tolerability to a 1 mL delivery of 5% dextrose immediately following delivery with the hMTS device and then at 10 min and 30 min post-delivery. Although the delivery site shows a whitish ring immediately following delivery, note that this is not the “raised white

tense papule” that others have associated with more conventional intradermal delivery such as the Manoux technique (15).

Upon removal of the hMTS patch after delivery, a small amount (1–3  $\mu$ L) of formulation is typically observed on the surface of the skin. When this fluid is removed by gentle wiping with a tissue, no additional fluid is observed. A pinkish blotch, the size of the hMTS array, is typically seen upon patch removal, but the blotch fades so as to become nearly indistinguishable within 5 min. A small dome, again approximately the size of the hMTS array, was observed on the swine skin as well. The dome yielded but did not “leak” under gentle pressure. The dome was resolved, both visually and by touch, within 40 min of removing the application patch.

### Pharmacokinetics—*In-Vivo* Naloxone Delivery

In an effort to better characterize the delivery, a 1 mg/mL commercial formulation of naloxone was infused into the swine using the hMTS POC device. Naloxone is a  $\mu$ -opioid receptor competitive antagonist used primarily to combat overdose of drugs such as heroin. Typically administered intravenously for fast response, naloxone is only about 2% bioavailable when administered orally. Naloxone is well-absorbed but is nearly 90% removed during first pass. Literature review indicates that the half-life of naloxone in human adults is 30–81 min and considerably longer (approx. 3 h) in children. Naloxone is excreted in the urine as metabolites (16). In this study, naloxone is used as a marker drug and was not chosen for any therapeutic value.

**Table 1** Summary of DOP Data Collected in Either Hairless Guinea Pigs or Domestic Swine (standard deviation and relative standard deviation refer to intra-array variability)

	500 $\mu$ m structures in HGPs	500 $\mu$ m structures in Swine (ham)	900 $\mu$ m structures in Swine (ham)
Number of measurements	108	108	288
Average ( $\mu$ m)	210 $\mu$ m	250 $\mu$ m	612 $\mu$ m
Standard deviation ( $\mu$ m)	30 $\mu$ m	40 $\mu$ m	99 $\mu$ m
Relative standard deviation	15%	16%	16%

**Fig. 4** Images of intradermal infusion of a 0.05% methylene blue formulation in swine at  $T=0$  and  $T=9$  min post-patch removal. Note that skin is dry to the touch.



Three different animals were used for the study comparing the PK profiles generated after hMTS infusion and subcutaneous injection. A comparative graph of naloxone blood levels *versus* time by delivery route is shown in Fig. 6.

The areas under the curves (AUCs) associated with the average PK profile for each group are similar. When delivered via subcutaneous injection, naloxone has a very rapid  $T_{max}$  (10 min). In each trial, the  $T_{max}$  for the profile resulting from hMTS administration of naloxone occurred at 30 min; the relatively slow  $T_{max}$  is not surprising given that the 1 mL hMTS administration took more than 5 min to complete.

Figure 7 shows the hMTS delivery site 10 min post-delivery of 1 mL of naloxone hydrochloride.

Following delivery of the naloxone hydrochloride formulation, the site of application is slightly raised and may show a white ring for the first minute or two following delivery; this quickly fades. The site remains slightly pink for 10–15 min after delivery is complete.

#### Pharmacokinetics—*In-Vivo* hGH Delivery

Human growth hormone (hGH) is a polypeptide hormone with a molecular weight of approximately 22 kDa. Ther-

apeutically, hGH is used to treat a number of conditions including chronic renal failure, Turner syndrome and growth failure in children, during which it may be administered as a daily injection. Like most proteins, hGH is not readily compatible with oral administration (12).

Two groups of three similarly sized swine were administered hGH either by the hMTS device or via subcutaneous injection. Blood samples, collected at specified time points through an 8-h period, were analyzed for hGH. Comparative PK profiles were generated and are shown in Fig. 8.

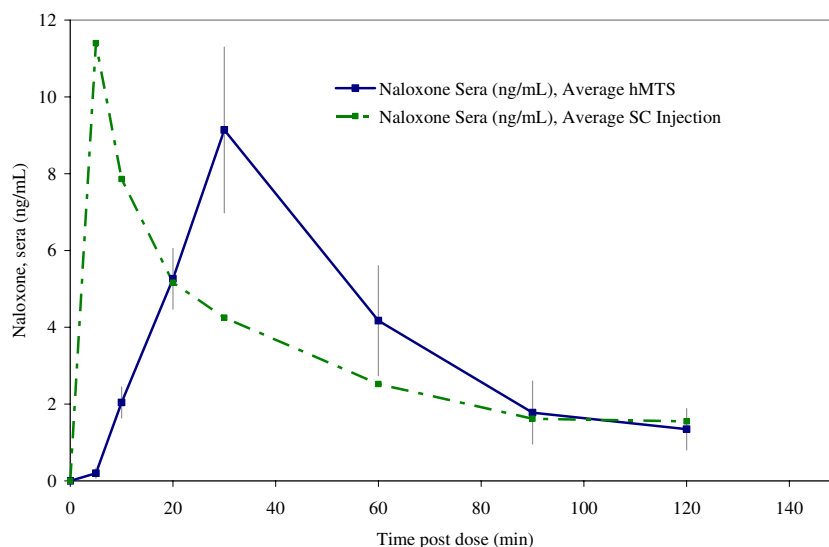
#### Pharmacokinetics—*In-Vivo* ETAT Delivery

The ETAT formulation was developed in an effort to design a PK model for monoclonal antibody therapies. The polyclonal ETAT fraction provides measurable activity (binding to tetanus toxoid) and specificity (detection with an anti-equine conjugate), thus verifying stability of the IgG molecule, and is a reasonable model for a monoclonal antibody administration. Most monoclonal antibodies are administered *via* injection or infusions once a week, once a month or once every other month. This class of therapeutics is generally not compatible with oral administration as they are destroyed in the digestive system (12). ETAT was formulated at 57 mg IgG /mL, a concentration similar to



**Fig. 5** Series of images 0, 10 and 30 min post-delivery of 1 mL of dextrose.

**Fig. 6** Comparative PK profiles in swine administered 0.7–1 mL of 1 mg/mL commercial naloxone hydrochloride formulation via hMTS ( $n=3$  per group) or subcutaneous injection ( $n=1$ ); blood levels are adjusted for dose delivered.



certain marketed mAb products. The comparative PK profiles (hMTS *versus* subcutaneous injection) are presented in Fig. 9.

## DISCUSSION

The AUCs associated with the hMTS delivery of both naloxone and hGH are essentially equivalent to those resulting from subcutaneous administration. Interestingly, in both cases, the  $T_{max}$  is different between the two delivery methods. For naloxone, the delayed  $T_{max}$  (relative to injection) is likely due to the delivery time *versus* the time required for this small molecule to be absorbed systemically. The delivery time associated with the hMTS administration of naloxone hydrochloride was between 5–10 min (depend-

ing on the trial), very similar to the  $T_{max}$  associated with the injection.

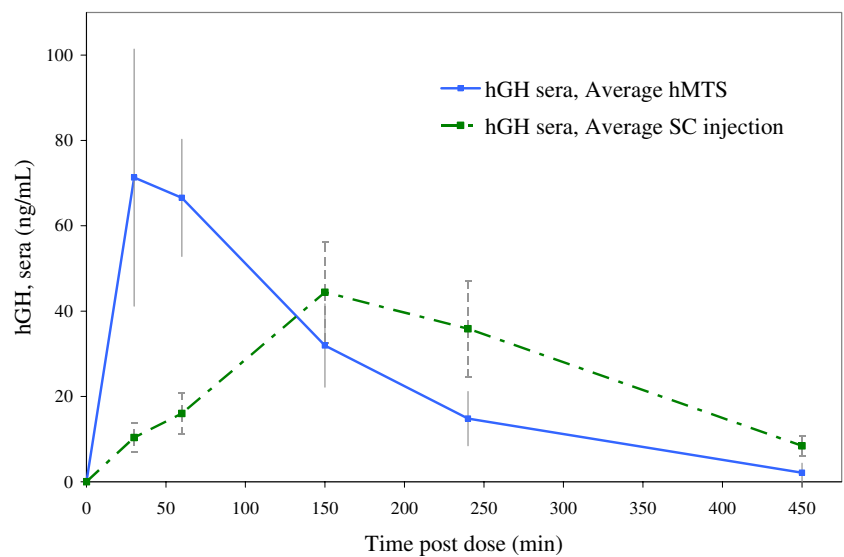
In the case of hGH, the hMTS administration profile reached  $T_{max}$  at either 30 or 60 min, while the profiles resulting from administrations conducted by subcutaneous injection all reached  $T_{max}$  at the 150 min time point. Although not statistically significant, the  $C_{max}$  for hMTS administration is higher than the  $C_{max}$  measured from the profiles generated following subcutaneous injection. These differences may be attributed to the faster transport of the macromolecule to the systemic circulation through the highly vascularized intradermal tissue rather than through the more dense subcutaneous tissue. Specifically, the lymphatic capillaries, abundant in the dermis, may be the primary source of uptake within the intradermal space. The lymphatic capillaries are larger than blood vessels found adjacent and are designed for rapid uptake and transport of large molecules. The lymphatic capillaries form a specialized system of microvasculature to regulate interstitial fluid pressure through a series of one-way valves or junctions (17, 18). It seems possible that the early  $T_{max}$  and high  $C_{max}$  observed in the hMTS hGH PK profile may be attributed to primary absorption of the drug by the lymphatic capillaries rather than by the blood vessels, which may more commonly provide uptake in subcutaneous injections. Utilizing this lymphatic pathway, intradermal delivery may provide faster access to the systemic circulation, especially for large molecule therapeutics.

The AUC associated with the hMTS administration is very similar to that resulting from the subcutaneous injection of the protein formulation. Unfortunately, the first blood sample collected in this study was at 2 h post-delivery. If the ETAT achieved faster absorption into the systemic circulation via the lymphatic capillaries, as



**Fig. 7** Typical hMTS Delivery Site (swine) 10 min after administration of 1 mL of Naloxone Hydrochloride.

**Fig. 8** Comparative PK profiles in swine ( $n=3$  per group) administered 0.75 mL of 2 mg/mL hGH formulated with 5% dextrose in water and administered via either hMTS or subcutaneous injection.



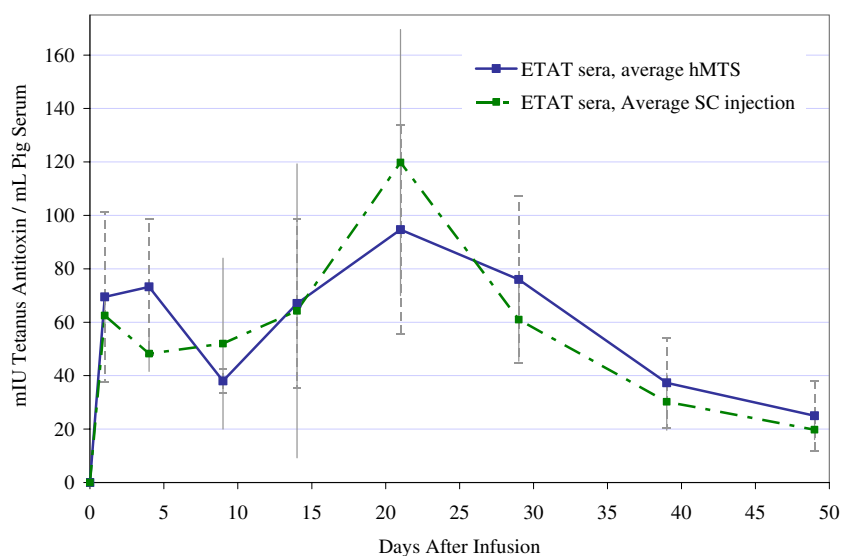
proposed above, the  $C_{max}$  associated with the profile may have passed before the first blood sample was collected. It appears that ETAT administered via hMTS follows expected elimination kinetics, even over the course of several weeks.

## CONCLUSIONS

The 3M hMTS can provide rapid transdermal delivery of liquid formulations up to 1,500  $\mu$ L, providing an option for administration for molecules not typically compatible with transdermal delivery. The strength and flex modulus of the structures prevents the microneedles from fracturing or breaking under impact forces several times higher than those

created upon application. The structures penetrate the stratum corneum cleanly and reproducibly and provide delivery at rates up to 300  $\mu$ L/min 250–600  $\mu$ m beneath the surface of the skin. Deliveries of a small molecule salt, a protein and a model monoclonal antibody, molecules not compatible with traditional transdermal delivery, were achieved with measured PK profiles and relative bioavailabilities similar to what are observed following subcutaneous injection of these same formulations. Large molecules may actually access the systemic circulation faster when introduced intradermally rather than via injection. The 3M hMTS demonstrates relatively fast (5–20 min) and very efficient transdermal delivery of large volumes of liquid formulations. The skin shows good tolerability to the hMTS deliveries and recovers with no long-term edema or erythema.

**Fig. 9** Comparative PK profiles in swine ( $n=4$  per group) administered 1 mL of 57 mg/mL ETAT formulated in 4.25% Dextrose, 75 mM NaCl and administered via either hMTS or subcutaneous injection.



## ACKNOWLEDGEMENTS

The authors acknowledge the many contributions of K. Puckett, J. Oesterich, R. Krienke, D. Heidebrink, P. Young, C. Webb, and M. Hopp

**Open Access** This article is distributed under the terms of the Creative Commons Attribution Noncommercial License which permits any noncommercial use, distribution, and reproduction in any medium, provided the original author(s) and source are credited.

## REFERENCES

1. Bronaugh RL, Maibach HI. Percutaneous absorption: drugs-cosmetics-mechanisms-methodology. New York: Dekker; 1999.
2. Guy RH, Hadgraft J. Transdermal drug delivery. 2nd ed. New York: Dekker; 2003.
3. Prausnitz MR. Microneedles for transdermal drug delivery. *Adv Drug Deliv Rev.* 2004;56:581–7.
4. Haq MI, Edwards C, Kalavala M, Anstey A, Morrissey A, John D, *et al.* Clinical administration of microneedles: skin puncture, pain and sensation. *Biomed Microdevices.* 2009; 11:35–47.
5. Mikszta JA, Alarcon JB, Brittingham JM, Sutter DE, Pettis RJ, Harvey NG. Improved genetic immunization via micromechanical disruption of the skin-barrier function and targeted epidermal delivery. *Nat Med.* 2002;8:415–9.
6. McAllister DV, Wang PM, Davis SP, Park J, Canatella PJ, Allen MG, *et al.* Microfabricated needles for transdermal delivery of macromolecules and nanoparticles: fabrication methods and transport studies. *PNAS.* 2003;100:13755–60.
7. Nordquist L, Roxhed N, Griss P, Stemme G. Novel microneedle patches for active insulin delivery are efficient in maintaining glycaemic control: an initial comparison with subcutaneous administration. *Pharm Res.* 2007;24:1381–8.
8. Van Damme P, Oosterhuis-Kafeja F, Van der Wielen M, Almagor Y, Sharon O, Levin Y. Safety and efficacy of a novel microneedle based dose sparing intradermal influenza vaccination in healthy adults. *Vaccine.* 2009;27:454–9.
9. Gupta J, Felner EI, Prausnitz MR. Minimally invasive insulin delivery in subjects with type 1 diabetes using hollow microneedles. *Diab Technol Ther.* 2009;11:329–37.
10. “Delivery Mechanisms for Large Molecule Drugs, Successes and failures of leading technologies and key drivers for market success”; Fraser-Moodie, Isabel. Business Insights Ltd, 2008
11. Standard & Poor’s Industry Surveys Biotechnology; Silver, Steven, Feb 2009
12. Lee HJ. Protein drug oral delivery: the recent progress. *Arch Pharm Res.* 2008;25:572–84.
13. Davis SP, Landis BJ, Adams ZH, Allen MG, Prausnitz MR. Insertion of microneedles into skin: measurement and prediction of insertion force and needle fracture force. *J Biomech.* 2004;37:115–6.
14. Swindle MM, Smith AC. Comparative anatomy and physiology of the swine. *Scand J Lab Anim Sci.* 1998;25:11–21.
15. Laurent PE, Bonnet S, Alchas P, Regolini P, Mikszta JA, Pettis R, *et al.* Evaluation of the clinical performance of a new intradermal vaccine administration technique and associated delivery system. *Vaccine.* 2007;25:883–884.
16. Liu M, Wittbrodt E. Low-dose oral naloxone reverses opioid-induced constipation and analgesia. *J Pain Symptom Manage.* 2002;23:48–53.
17. Leak L. Studies on the permeability of lymphatic capillaries. *J Cell Biol.* 1971;50:300–23.
18. Pepper MS, Skobe M. Lymphatic endothelium: morphological, molecular and functional properties. *J Cell Biol.* 2003;163:209–13.